*Structural Engineering and Mechanics, Vol. 29, No. 3 (2008) 241-258*
DOI: http://dx.doi.org/10.12989/sem.2008.29.3.241


# Identification of prestress force in a prestressed Timoshenko beam

Z. R. Lu† and J. K. Liu‡

*School of Engineering, Sun Yat-sen University, Guangzhou 510275, P. R. China*

S. S. Law‡†

*Civil and Structural Engineering Department, The Hong Kong Polytechnic University, Hunghom, Kowloon, Hong Kong, P. R. China*

*(Received December 15, 2006, Accepted March 24, 2008)*

**Abstract.** This paper presents a new identification approach to prestress force. Firstly, a bridge deck is modeled as a prestressed Timoshenko beam. The time domain responses of the beam under sinusoidal excitation are studied based on modal superposition. The prestress force is then identified in the time domain by a system identification approach incorporating with the regularization of the solution. The orthogonal polynomial function is used to improve the noise effect and obtain the derivatives of modal responses of the bridge. Good identification results are obtained from only the first few measured modal data under both sinusoidal and impulsive excitations. It is shown that the proposed method is insensitive to the magnitude of force to be identified and can be successfully applied to indirectly identify the prestress force as well as other physical parameters, such as the flexural rigidity and shearing rigidity of a beam even under noisy environment.

**Keywords:** identification; prestress force; time domain; vibration.

## 1. Introduction

Prestress force has been used very often in long span structures, and it is one of the most important factors to describe the load-carrying capacity of a structure. Interests in the safety assessment of the existing prestressed concrete bridges have been increased in recent years. A quick and non-destructive test method to assess the condition of the prestress force in the structure is required for its maintenance program.

Work has been done on the identification of prestress force in a Bernoulli-Euler beam (Law and Lu 2005). In practice lots of bridges have large cross-section, so the effects of rotatory inertia and shear deformation must be taken into account. The aim of this paper is therefore to address the problem of prestress force identification in a bridge deck that can be modeled as a simply supported

† Ph.D., Corresponding author, E-mail: zhongronglv@163.com
‡ Professor, E-mail: Liujike@mail.sysu.edu.cn
‡† Associate Professor, E-mail: cesslaw@polyu.edu.hk

Timoshenko beam. The bridge deck may lose some of its prestress force due to creep with long period of service under design or overloaded vehicles. A large reduction of the prestress force from the design value could lead to serviceability and safety problems. Therefore assessment on the magnitude of the prestress force or the loss of pretress force in the bridge deck is important for its load-carrying capacity. However the existing prestress force cannot be estimated directly unless the bridge deck has been instrumented at the time of construction. Several researchers (Abraham *et al.* 1995) tried to predict the loss of prestress force based on a damage index derived from the derivatives of mode shapes. Others (Miyamoto *et al.* 2000) studied the behavior of a beam with unbonded tendons, and a formula was proposed to predict the modal frequency for a given prestress force with laboratory and field test verifications. Saiidi *et al.* (1994) reported a study that the sensitivity of modal frequency decreases with higher vibration modes, and the prestress force affects the first few lower modes more significantly than the higher ones. Consequently the prestress force would be difficult to identify from the modal frequencies. Abraham *et al.* (1995) also reported that the mode shapes remain almost identical with different prestress force in the beam, and it will also be difficult to identify the force from the measured mode shapes. More recently, Kim *et al.* (2004) proposed a nondestructive method to detect prestress-loss in beam-type PSC bridges using a few natural frequencies. An inverse-solution algorithm is proposed to detect the prestress-loss by measuring the changes in natural frequencies, and the prestress loss in a two-span continuous PSC beams has been identified successfully.

In the present work, the dynamic response of a prestressed Timoshenko beam is studied based on modal superposition method. An inverse problem to identify the prestress force is then formulated. The prestress force, flexural rigidity and shearing rigidity of the beam are all included in the identification equation in time domain. Considering that the inverse problem always yields unbounded results due to the non-continuity of the dependence of the results on the measured responses, the damped least squares method is adopted to smooth out the large variations in the identified prestress force. Orthogonal polynomial function (Law and Zhu 2000) is used to approximate the measured strain responses to remove the measurement noise effect. The effectiveness of using an impulsive force in the identification is also illustrated. The magnitude of prestress force that can be identified is studied and the recommendation is made for the identification of very small prestress forces. The effectiveness of the proposed method was verified from both numerical study and experimental work. The works reported illustrated that identification of prestress force with normal modal testing technique is feasible even with noisy data.

## 2. Forward problem

### 2.1 Differential equation of motion

The bridge deck is modeled as a simply supported uniform prestressed Timoshenko beam subjected to an external excitation force $P(t)$ acting at a distance $x_p$ from the left support as shown in Fig. 1. The coupled equation for the total deflection $y$ and rotation $\psi$ of the cross-section under a compressive axial force $T_p$ can be written as

$$\rho A\frac{\partial^2 y(x,t)}{\partial t^2}+c\frac{\partial y(x,t)}{\partial t}-kAG\left(\frac{\partial^2 y}{\partial x^2}-\frac{\partial \psi}{\partial x}\right)+T_p\frac{\partial^2 y(x,t)}{\partial x^2}=P(t)\delta(x-x_p) \tag{1}$$

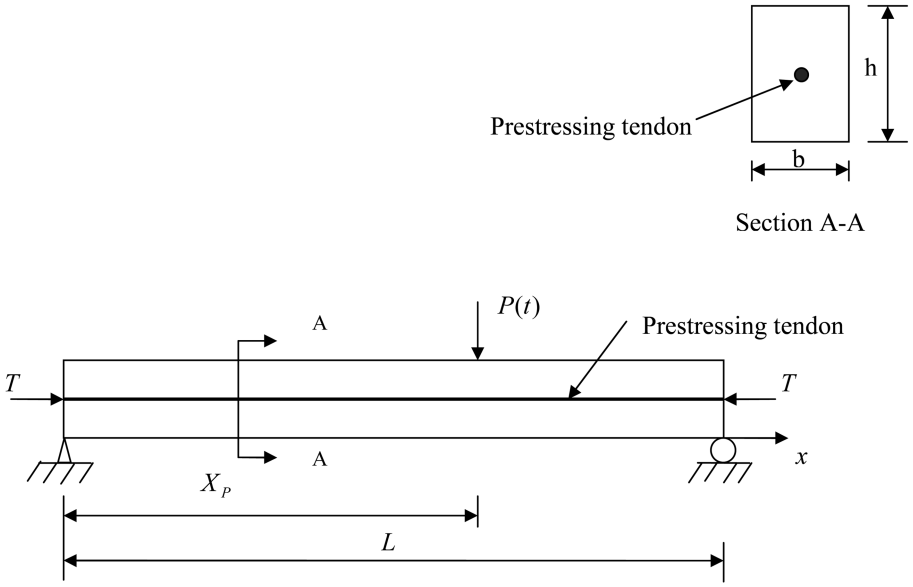


Fig. 1 The prestressed Timoshenko beam model

$$\rho I\frac{\partial^2 \psi}{\partial x^2} - kAG\left(\frac{\partial y}{\partial x} - \psi\right) - EI\frac{\partial^2 \psi}{\partial x^2} = 0 \tag{2}$$

where $y$ is the total deflection due to bending and shear, $\psi$ is the slope of deflection due to bending, $\rho$ is the mass density of the beam, $A$ is the cross-sectional area, $c$ is the viscous damping coefficient, $E$ is the Young's modulus, $G$ is the shear modulus, $k$ is the shear coefficient of cross-section, $I$ is the moment of inertia of the beam cross-section, $T_p$ is the externally applied compressive axial force (note that compression is positive and tension is negative), $\delta(x)$ is the Dirac delta function and $P(t)$ is the external excitation.

### 2.2 Modal responses

The kinetic energy $T$, the strain energy $U$, the work done $W_{Tp}$ due to the prestress force, the work done $W_c$ due to the viscous damping in the beam, and the work done $W$ due to the external force can be expressed respectively as

$$T = \frac{1}{2}\int_0^L \left[\rho A\left(\frac{\partial y(x,t)}{\partial t}\right)^2 + \rho I\left(\frac{\partial \psi(x,t)}{\partial t}\right)^2\right]dx \tag{3}$$

$$U = \frac{1}{2}\int_0^L \left[EI(x)\left(\frac{\partial^2 y(x,t)}{\partial x^2}\right)^2 + kGA\left(\frac{\partial y}{\partial x} - \psi\right)^2\right]dx \tag{4}$$

$$W_{Tp} = \frac{1}{2}\int_0^L T\frac{\partial^2 y(x,t)}{\partial x^2}dx \tag{5}$$

$$W_c = -\int_0^L y(x,t)c\frac{\partial y(x,t)}{\partial t}dx \tag{6}$$

$$W = \int_0^L P(t)\delta(x-x_p)y(x,t)dx \tag{7}$$

The vibration responses of the beam $y(x,t)$, $\psi(x,t)$ in modal co-ordinates can be expressed as

$$y(x,t) = \sum_{i=1}^{n} Y_i(x)q_i(t) \tag{8}$$

$$\psi(x,t) = \sum_{i=1}^{n} \phi_i(x)q_i(t) \tag{9}$$

where $Y_i(x), \phi_i(x)$ are the assumed vibration modes satisfying the boundary conditions, $q_i(t)$ is the generalized co-ordinates.

Substituting Eqs. (8) and (9) into Eqs. (3)-(7), we have

$$T = \frac{1}{2}\int_0^L \left[\rho A\left(\sum_{i=1}^{n} Y_i(x)\dot{q}_i(t)\sum_{j=1}^{n} Y_j(x)\dot{q}_j(t)\right) + \rho I\left(\sum_{i=1}^{n} \phi_i(x)\dot{q}_i(t)\sum_{j=1}^{n} \phi_j(x)\dot{q}_j(t)\right)\right]dx$$

$$= \frac{1}{2}\sum_{i=1}^{n}\sum_{j=1}^{n} \dot{q}_i(t)m_{ij}\dot{q}_j(t) \tag{10}$$

$$U = \frac{1}{2}\int_0^L \left[EI\left(\sum_{i=1}^{n} q_i(t)\,\phi_i'(x)\sum_{j=1}^{n} q_j(t)\phi_j'(x) + \right.\right.$$

$$\left.\left. kGA\left(\sum_{i=1}^{n} q_i(t)Y_i'(x) - \sum_{i=1}^{n} q_i(t)\phi_i(x)\right)\left(\sum_{j=1}^{n} q_j(t)Y_j'(x) - \sum_{j=1}^{n} q_j(t)\phi_j(x)\right)\right]dx$$

$$= \frac{1}{2}\sum_{i=1}^{n}\sum_{j=1}^{n} q_i(t)k_{ij}q_j(t) \tag{11}$$

$$W_{Tp} = \frac{1}{2}\int_0^L T\sum_{i=1}^{n} q_i(t)Y_i'(x)\sum_{j=1}^{n} q_j(t)Y_j'(x)dx = \sum_{i=1}^{n}\sum_{j=1}^{n} q_i(t)k_{ij}'q_j(t) \tag{12}$$

$$W_c = -\int_0^L c\sum_{i=1}^{n} Y_i(x)q_i(t)\sum_{j=1}^{n} Y_j(x)\dot{q}_j(t)dx = -\sum_{i=1}^{n}\sum_{j=1}^{n} q_i(t)c_{ij}\dot{q}_j(t) \tag{13}$$

$$W = \int_0^L P(t)\delta(x-x_p)\sum_{i=1}^{n} Y_i(x)q_i(t)dx = \sum_{i=1}^{n} P(t)Y_i(x_p)q_i(t) = \sum_{i=1}^{n} f_i(t)q_i(t) \tag{14}$$

where

$$m_{ij} = \int_0^L [\rho A Y_i(x)Y_j(x) + \rho I\phi_i(x)\phi_j(x)]dx$$

$$k_{ij} = \int_0^L [EI\phi_i'(x)\phi_j'(x) + kGA(Y_i'(x) - \phi_i(x))(Y_j'(x) - \phi_j(x))]dx$$

$$k_{ij}' = \int_0^L T_p Y_i'(x)Y_j'(x)dx$$

$$c_{ij} = \int_0^L cY_i(x)Y_j(x)dx, \quad f_i(t) = P(t)Y_i(x_p) \tag{15}$$

$\dot{q}_i(t)$ and $\phi_i'(x)$ denote the first derivative of $q_i(t)$ and $\phi_i(x)$ with respect to time $t$ and $x$, respectively. $m_{ij}$ is the generalized mass, $k_{ij}$ is the generalized stiffness and $f_i(t)$ is the generalized force. The Lagrange equation can be written as

$$\frac{d}{dt}\left(\frac{\partial T}{\partial \dot{q}}\right) - \frac{\partial T}{\partial q} + \frac{\partial U}{\partial q} - \frac{\partial W_{Tp}}{\partial q} - \frac{\partial W_c}{\partial q} = \frac{\partial W}{\partial q} \tag{16}$$

Substituting Eqs. (10)-(14) into Eq. (16), we have

$$\sum_{j=1}^{n} m_{ij}\ddot{q}_j(t) + \sum_{j=1}^{n} c_{ij}\dot{q}_j(t) + \sum_{j=1}^{n} (k_{ij} - k_{ij}')q_j(t) = f_i(t), \quad i = 1, 2, \ldots, n \tag{17}$$

Eq. (17) can be expressed in matrix form as

$$M\ddot{q}(t) + C\dot{q}(t) + (K - K')q(t) = F(t) \tag{18}$$

where

$$\begin{gathered} M = \{m_{ij}, i = 1, 2, \ldots, n;\ j = 1, 2, \ldots, n\}, \quad C = \{c_{ij}, i = 1, 2, \ldots, n;\ j = 1, 2, \ldots, n\} \\ K = \{k_{ij}, i = 1, 2, \ldots, n;\ j = 1, 2, \ldots, n\}, \quad K' = \{k_{ij}', i = 1, 2, \ldots, n;\ j = 1, 2, \ldots, n\} \\ q(t) = \{q_1(t), q_2(t), \ldots, q_n(t)\}^T, \quad F(t) = \{f_1(t), f_2(t), \ldots, f_n(t)\}^T \end{gathered} \tag{19}$$

### 2.2 Assumed mode shapes

The general form of the vibration modes for a uniform Timoshenko beam can be written as

$$Y(x) = A_1\cos(\alpha x) + A_2\sin(\alpha x) + A_3\sinh(\beta x) + A_4\cosh(\beta x) \tag{20}$$

$$\phi(x) = B_1\cos(\alpha x) + B_2\sin(\alpha x) + B_3\sinh(\beta x) + B_4\cosh(\beta x) \tag{21}$$

where $A_1$~$A_4$ and $B_1$~$A_4$ are arbitrary constants, $\alpha$ and $\beta$ are frequency parameters.

The vibration modes of a simply-supported Timoshenko beam are (Abramovich 1991)

$$Y_i(x) = A_i\sin\left(\frac{i\pi}{L}x\right) \tag{22}$$

$$\phi_i(x) = \cos\left(\frac{i\pi}{L}x\right) \tag{23}$$

where

$$A_i = \frac{i\pi L}{[(i\pi)^2 - p^2b^2]\left(1 - \frac{T_p}{a}\right)}, \quad a = kGA, \quad b^2 = \frac{EI}{aL^2}, \quad p^2 = \frac{(i\pi)^4 - (i\pi)^2\overline{k}^2}{1 + (i\pi)^2 D}$$

$$\overline{k}^2 = \frac{T_pL^2}{EI\left(1 - \frac{T_p}{a}\right)}, \quad D = R^2\left(1 - \frac{T_p}{a}\right) + b^2, \quad R^2 = \frac{I}{AL^2}$$

Then Eq. (18) can be reduced into the following form

$$\begin{bmatrix} m_{11} & 0 & \dots & 0 \\ 0 & m_{22} & \dots & 0 \\ & & \ddots & \\ 0 & 0 & \dots & m_{nn} \end{bmatrix} \begin{Bmatrix} \ddot{q}_1(t) \\ \ddot{q}_2(t) \\ \vdots \\ \ddot{q}_n(t) \end{Bmatrix} + \begin{bmatrix} 2m_1\xi_1\omega_1 & 0 & \dots & 0 \\ 0 & 2m_2\xi_2\omega_2 & \dots & 0 \\ & & \ddots & \\ 0 & 0 & \dots & 2m_n\xi_n\omega_n \end{bmatrix} \begin{Bmatrix} \dot{q}_1(t) \\ \dot{q}_2(t) \\ \vdots \\ \dot{q}_n(t) \end{Bmatrix} +$$

$$\begin{bmatrix} k_{11}-k'_{11} & 0 & \dots & 0 \\ 0 & k_{22}-k'_{22} & \dots & 0 \\ & & \ddots & \\ 0 & 0 & \dots & k_{nn}-k'_{nn} \end{bmatrix} \begin{Bmatrix} q_1(t) \\ q_2(t) \\ \vdots \\ q_n(t) \end{Bmatrix} = \begin{Bmatrix} f_1(t) \\ f_2(t) \\ \vdots \\ f_n(t) \end{Bmatrix} \tag{24}$$

The modal responses of the beam are computed in the time domain numerically using the Newmark's integration method (Newmark 1959). The natural frequency of the beam can be written as (Abramovich 1991)

$$\overline{\omega}_1 = \omega_0 \sqrt{\left(1 - \frac{T_p}{T_{cr}}\right) C_1} \tag{25}$$

where

$$C_1 = \frac{1 + \pi^2 R^2 \left(1 + \frac{E}{kG}\right)}{1 + \pi^2 R^2 \left(1 + \frac{E}{kG} - \frac{T_p}{a}\right)}, \quad \omega_0 = \left(\frac{i\pi}{L}\right)^2 \sqrt{\frac{EI}{\rho A}} \sqrt{\frac{1}{\left[1 + (i\pi)^2 \left(\frac{I}{AL^2} + \frac{EI}{kAGL^2}\right)\right]}}$$

$$T_{cr} = \frac{(\pi^2/L^2)}{[(1/EI) + (\pi^2/L^2 a)]}$$

## 3. Inverse problem

### 3.1 Identification of the prestress force from measured displacements

Express the measured displacements $\tilde{y}(x_m, t)$ at a point $x_m$ from the left support in modal co-ordinates

$$\tilde{y}(x_m, t) = \sum_{i=1}^{N} Y_i(x) q_i(t) \quad (m = 1, 2, \dots, N_m) \tag{26}$$

where $N_m$ is the number of measurement locations and $N$ is the number of measured modes in the responses. Eq. (26) can be written as

$$\{\tilde{y}\}_{N_m \times 1} = [Y]_{N_m \times N} \{q\}_{N \times 1} \tag{27}$$

where $\{y\}_{N_m\times 1}$ is the vector of displacements at $N_m$ measurement locations. The modal displacement can be written in the form of the least-squares pseudo-inverse

$$\{q\}_{N\times 1} = ([Y]^T_{N\times N_m}[Y]_{N_m\times N})^{-1}[Y]^T_{N\times N_m}\{\tilde{y}\}_{N_m\times 1} \tag{28}$$

The modal velocity and acceleration of the beam responses can be obtained from Eq. (28) by numerical methods. However, when the measurements are polluted by noise, the use of central difference method to calculate the modal velocity and acceleration may lead to large computational error. Therefore the generalized orthogonal polynomial (Law and Zhu 2000) is used to model the measured displacement so as to reduce error as

$$\tilde{y}(x_j,t) = \sum_i^{Nf} b_i T_i(t) \tag{29}$$

where $\tilde{y}(x_j,t)$ is the approximate displacement at the $j$th measuring point. $N_f$ is the order of the orthogonal polynomial function. The velocity and acceleration are then approximated by the first and second derivatives of the orthogonal polynomial.

Rewriting Eq. (29) in matrix form, we have

$$\begin{aligned}\{\tilde{y}\}_{N_m\times 1} &= [B]_{N_m\times Nf}[T]_{Nf\times 1}\\ \{\dot{\tilde{y}}\}_{N_m\times 1} &= [B]_{N_m\times Nf}[\dot{T}]_{Nf\times 1}\\ \{\ddot{\tilde{y}}\}_{N_m\times 1} &= [B]_{N_m\times Nf}[\ddot{T}]_{Nf\times 1}\end{aligned} \tag{30}$$

where $[B]_{N_m\times Nf}, [T]_{Nf\times 1}, [\dot{T}]_{Nf\times 1}, [\ddot{T}]_{Nf\times 1}$ are the coefficient matrix of the polynomial, the orthogonal polynomial matrix, the first and second derivatives of the orthogonal polynomial variable matrixes, respectively. The coefficient matrix $[B]$ can be obtained from Eq. (30) by the least-squares method

$$[B]_{N_m\times Nf} = \{\tilde{y}\}_{N_m\times 1}[T]^T_{1\times Nf}([T]_{Nf\times 1}[T]^T_{1\times Nf})^{-1} \tag{31}$$

Substituting matrix $[B]$ into Eq. (30), we can obtain $\{\dot{\tilde{y}}\}$ and $\{\ddot{\tilde{y}}\}$. And substituting $\{\tilde{y}\}, \{\dot{\tilde{y}}\}, \{\ddot{\tilde{y}}\}$ and the derivatives of $[T]$ into Eq. (28), we can obtain the modal displacement $\boldsymbol{q}$, modal velocity $q$ and modal acceleration $\dot{q}$. Substituting $q$, $\dot{q}$ and $\ddot{q}$ into Eq. (24), and after transformation, we have

$$[K']\{q(t)\} = [M]\{\ddot{q}(t)\} + [C]\{\dot{q}(t)\} + [K]\{q(t) - F(t)\} \tag{32}$$

where matrix $[K']$ contains the prestress force $T$ which is assumed constant throughout the length of the beam, matrix $[C]$ contains the modal damping $\xi_i$ and frequency $\omega_i$ which are assumed unchanged with time, and matrix $[K]$ contains the system parameters of the beam which are also assumed unchanged.

The inverse problem is to solve Eq. (32) in the time domain to obtain the prestress force $T_p$. Rewrite Eq. (32) in a compact form

$$\{H\}_{n\times 1}T_p = \{G\}_{n\times 1} \tag{33}$$

where

$$\{H\} = \begin{bmatrix} k_{T11} & 0 & \dots & 0 \\ 0 & k_{T22} & \dots & 0 \\ 0 & 0 & \ddots & 0 \\ 0 & 0 & \dots & k_{Tnn} \end{bmatrix}_{n\times n} \begin{Bmatrix} q_1(t) \\ q_2(t) \\ \vdots \\ q_n(t) \end{Bmatrix}_{n\times 1}$$

where $k_{Tii} = \int_0^L Y_i' Y_i' dx$ and vector $[G]$ contains all the terms on the right-hand-side of Eq. (32).

The prestress force $T_p$ can be calculated directly by the simple least-squares (LS) method

$$T_p = (\{H\}^T\{H\})^{-1}\{H\}\{G\} \tag{34}$$

In order to have bounds on the ill-conditioned solution, the damped least-squares (DLS) method is used and singular value decomposition is used in the pseudo-inverse computation. Eq. (34) can be written in the following form using the DLS method

$$T_p = (\{H\}^T\{H\} + \lambda I)^{-1}\{H\}\{G\} \tag{35}$$

Where $\lambda$ is a non-negative damping coefficient governing the contribution of the least-squares error in the solution. The solution of Eq. (35) is equivalent to minimizing the function

$$J(T_p, \lambda) = \min(\|\{H\}T_p - \{G\}\|^2 + \lambda\|T_p\|^2) \tag{36}$$

with the second term in Eq. (36) providing bounds to the solution.

### 3.2 Identification of press force from measured strains

The strain at the bottom of the beam at a point $x_m$ from the left support can be expressed similar to Eq. (26) in terms of the generalized co-ordinates as

$$\tilde{\varepsilon}(x_m, t) = -\frac{h_0}{2}\sum_{i=1}^{N} \phi'(x_m) q_i(t), \quad (m = 1, 2, \dots, N_m) \tag{37}$$

where $h_o$ is the depth of the beam. Eq. (37) can be written as

$$\{\tilde{\varepsilon}\}_{N_m\times 1} = [\phi']_{N_m\times N}\{q\}_{N\times 1} \tag{38}$$

where $\{\tilde{\varepsilon}\}_{N_m\times 1}$ is the vector of strains at $N_m$ measurement locations. Again the strain at the $j$th measuring point can be approximated by the orthogonal function $T(t)$ as

$$\tilde{\varepsilon}(x_j, t) = \sum_{i}^{Nf} b_i T_i(t) \tag{39}$$

The rest of the computation in the identification is similar to that for identification from measured displacements mentioned above.

### 3.3 Identification of prestress force, flexural rigidity and shear rigidity

Other variables in the system should be also included in the identification in reality. Since the dimensions of the beam can be measured accurately and the modal damping can be estimated from a preliminary spectral analysis before the identification, the variables subjected to variations are the flexural rigidity $EI$ and the shear rigidity $kGA$ of the beam section. If a uniform uncracked beam is considered in the problem, then we have $T_p$, $EI$ and $kGA$ as the three variables in the identification. Rewrite Eq. (32) as

$$\left( T_p \begin{bmatrix} k_{T11} & 0 & \dots & 0 \\ 0 & k_{T22} & \dots & 0 \\ 0 & 0 & \ddots & 0 \\ 0 & 0 & \dots & k_{Tnn} \end{bmatrix}_{n\times n} - EI \begin{bmatrix} k_{B11} & 0 & \dots & 0 \\ 0 & k_{B22} & \dots & 0 \\ 0 & 0 & \ddots & 0 \\ 0 & 0 & \dots & k_{Bnn} \end{bmatrix}_{n\times n} - kGA \begin{bmatrix} k_{S11} & 0 & \dots & 0 \\ 0 & k_{S22} & \dots & 0 \\ 0 & 0 & \ddots & 0 \\ 0 & 0 & \dots & k_{Snn} \end{bmatrix}_{n\times n} \right) \begin{Bmatrix} q_1(t) \\ q_2(t) \\ \vdots \\ q_n(t) \end{Bmatrix}$$

$$= \begin{bmatrix} m_{11} & 0 & \dots & 0 \\ 0 & m_{22} & \dots & 0 \\ 0 & 0 & \ddots & 0 \\ 0 & 0 & \dots & m_{nn} \end{bmatrix}_{n\times n} \begin{Bmatrix} \ddot{q}_1(t) \\ \ddot{q}_2(t) \\ \vdots \\ \ddot{q}_n(t) \end{Bmatrix}_{n\times 1} + \begin{bmatrix} 2m_1\xi_1\omega_1 & 0 & \dots & 0 \\ 0 & 2m_2\xi_2\omega_2 & \dots & 0 \\ 0 & 0 & \ddots & 0 \\ 0 & 0 & \dots & 2m_n\xi_n\omega_n \end{bmatrix}_{n\times n} \begin{Bmatrix} \dot{q}_1(t) \\ \dot{q}_2(t) \\ \vdots \\ \dot{q}_n(t) \end{Bmatrix}_{n\times 1} - \begin{Bmatrix} f_1(t) \\ f_2(t) \\ \vdots \\ f_n(t) \end{Bmatrix}_{n\times 1} \tag{40}$$

where $k_{Bii}$ and $k_{Sii}$ are components of $k_{ij}$ in Eq. (15).

The inverse problem is to solve Eq. (40) in the time domain to obtain the prestress force $T_p$, the flexural rigidity $EI$ and the shear rigidity $kGA$ which are decoupled in Eq. (40). Rewrite Eq. (40) in a simple form

$$[H]X = \{S\}_{n\times 1} \tag{41}$$

where

$$H = \begin{bmatrix} H_T & & \\ & H_{EI} & \\ & & H_{kGA} \end{bmatrix}, \quad X = \begin{Bmatrix} T_p \\ EI \\ kGA \end{Bmatrix}, \quad \{H_T\} = \begin{bmatrix} k_{T11} & 0 & \dots & 0 \\ 0 & k_{T22} & \dots & 0 \\ 0 & 0 & \ddots & 0 \\ 0 & 0 & \dots & k_{Tnn} \end{bmatrix}_{n\times n} \begin{Bmatrix} q_1(t) \\ q_2(t) \\ \vdots \\ q_n(t) \end{Bmatrix}_{n\times 1}$$

$$\{H_{EI}\} = \begin{bmatrix} k_{B11} & 0 & \dots & 0 \\ 0 & k_{B22} & \dots & 0 \\ 0 & 0 & \ddots & 0 \\ 0 & 0 & \dots & k_{Bnn} \end{bmatrix}_{n\times n} \begin{Bmatrix} q_1(t) \\ q_2(t) \\ \vdots \\ q_n(t) \end{Bmatrix}_{n\times 1}, \quad \{H_{kGA}\} = \begin{bmatrix} k_{S11} & 0 & \dots & 0 \\ 0 & k_{S22} & \dots & 0 \\ 0 & 0 & \ddots & 0 \\ 0 & 0 & \dots & k_{Snn} \end{bmatrix}_{n\times n} \begin{Bmatrix} q_1(t) \\ q_2(t) \\ \vdots \\ q_n(t) \end{Bmatrix}_{n\times 1}$$

and $\{S\}$ represents all the terms on the right-hand-side of Eq. (40).

Again $T_p$, $EI$ and $kGA$ can be calculated directly by the simple LS method

$$X = ([H]^T[H])^{-1}[H]^T[S] \tag{42}$$

or by the DLS method

$$X = ([H]^T[H] + \lambda I)^{-1}[H]\{S\} \tag{43}$$

## 4. Simulation and results

### 4.1 The prestress beam

A 20 m long simply supported Timoshenko beam with an axial prestress force of $0.1T_{cr}$ = $1.056 \times 10^7$ N or $0.3T_{cr} = 3.1677 \times 10^7$ N is studied. The parameters of the beam are: $\rho A = 5.0 \times 10^3$ kg/m, $E = 5 \times 10^{10}$ N/m$^2$, $L = 20$ m, $b = 0.6$ m, and $h_0 = 1.2$ m. The first six natural frequencies of the beam are: 3.442, 13.521, 29.560, 50.607, 75.621, 103.621 (Hz) and 3.036, 11.925, 26.070, 44.633, 66.695, 91.389 (Hz) for the two prestress states, respectively. The damping ratios for these six modes are all assumed to be 0.02. The prestress force is constant along the beam. The external exciting force is

$$f(t) = 8000[1 + 0.1\sin(10\pi t) + 0.05\sin(40\pi t)]N$$

acting at 7 m from the left support to excite the lower few modes.

### 4.2 Identification of the prestress force alone

White noise is added to simulate the polluted measurements as follows

$$y = y_{calculated} + Ep * N_{oise} * \mathrm{var}(y_{calculated})$$

$$\varepsilon = \varepsilon_{calculated} + Ep * N_{oise} * \mathrm{var}(\varepsilon_{calculated})$$

where $y$ and $\varepsilon$ are the vectors of polluted displacement and strain respectively, $Ep$ is the noise level, $N_{oise}$ is a standard normal distribution vector with zero mean and unit standard deviation, var($\bullet$) is the variance of the time history, $y_{calculated}$ and $\varepsilon_{calculated}$ are the vectors of calculated displacement and strain respectively. 5% and 10% noise levels are considered.

The first three modes are used in the calculation. Measured displacements at $1/4L$, $1/2L$ and $3/4L$ are used in the identification. The magnitude of the prestress force is $0.3T_{cr} = 3.1677 \times 10^7 N$. The sampling frequency is 1000 Hz, which is larger than two times the highest frequency of interest at 103.621 Hz. The beam is assumed to be at rest initially.

Fig. 2 shows the identified results from measured strains with 5% and 10% noise levels. There is only a slight difference in the time histories of the identified prestress in the two cases. This is because the measurements have been approximated with 20 terms of the orthogonal functions and the velocities and accelerations are subsequently obtained by directly differentiating the functions. This shows that the orthogonal function approach is effective in eliminating the noise in the measured data.

The large responses at the start and end of the time histories are typically ill-solutions in the problem due to the discontinuity of the solution in time at these two moments.

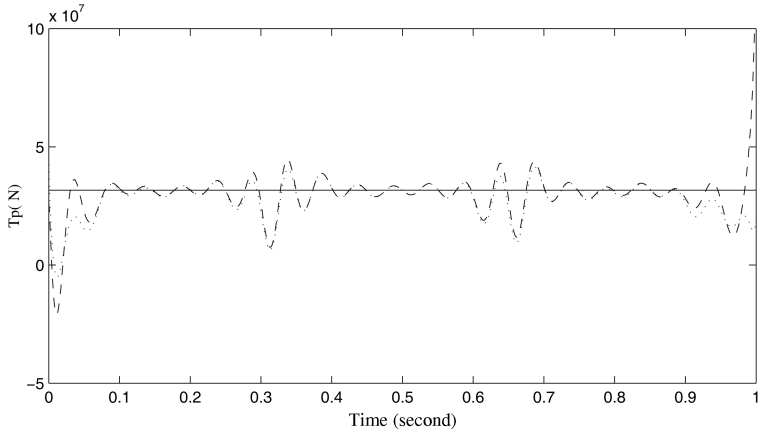


Fig. 2 Prestress force identified from three modes (—— True, ····· Identified 5% noise, ----- Identified 10% noise)

### *4.3 Sensitivity of proposed method to magnitude of prestress force*

In most cases of construction with prestress, the prestress force in a beam component is relatively small. A study is therefore made to analyze the errors involved in such identification with different magnitude of prestress force under different noise levels. The same beam and excitation as the above study are used. Five prestress levels and three noise levels are studied and the summation of errors of the identified force and the error expressed as $error = \|T_{pid} - T_{ptrue}\| / \|T_{ptrue}\| \times 100\%$ are shown in Table 1. The time histories of the identified prestress force which are $0.01T_{cr}$, $0.1T_{cr}$ and $0.3T_{cr}$ under 10% noise levels are shown in Fig. 3.

It is found from Table 1 that the noise level is not a significant factor. It seems that a small prestress force would include large relative percentage error in the identification. However, Fig. 3 shows that all the curves are fluctuating around their corresponding true prestress values except those close to the starting and end points. The total summation errors for the three curves are almost the same. That indicates the effectiveness of the proposed method is insensitive to the level of prestress force to be identified. Large relative percentage error is due to the small valve of the denominator when magnitude of the prestress force is small. Furthermore, the central ninety percentage of the force time history will give (nearly) true values of the force with smaller fluctuations.

Table 1 Error percentage in the identified force

| Prestress force | 1% noise | 5% noise | 10% noise |
|---|---|---|---|
| $0.01T_{cr}$ | $172.6/(8.12 \times 10^7)$ | $184.0/(9.36 \times 10^7)$ | $190.7/(1.03 \times 10^8)$ |
| $0.05T_{cr}$ | $77.87/(1.77 \times 10^8)$ | $78.8/(2.23 \times 10^8)$ | $83.89/(2.64 \times 10^8)$ |
| $0.1T_{cr}$ | $43.2/(2.06 \times 10^8)$ | $43.89/(2.14 \times 10^8)$ | $46.32/(2.47 \times 10^8)$ |
| $0.2T_{cr}$ | $25.76/(2.57 \times 10^8)$ | $28.13/(3.09 \times 10^8)$ | $29.24/(3.59 \times 10^8)$ |
| $0.3T_{cr}$ | $17.05/(2.54 \times 10^8)$ | $17.3/(3.21 \times 10^8)$ | $19.16/(4.06 \times 10^8)$ |

Note: (•) denotes the sum of squares error.

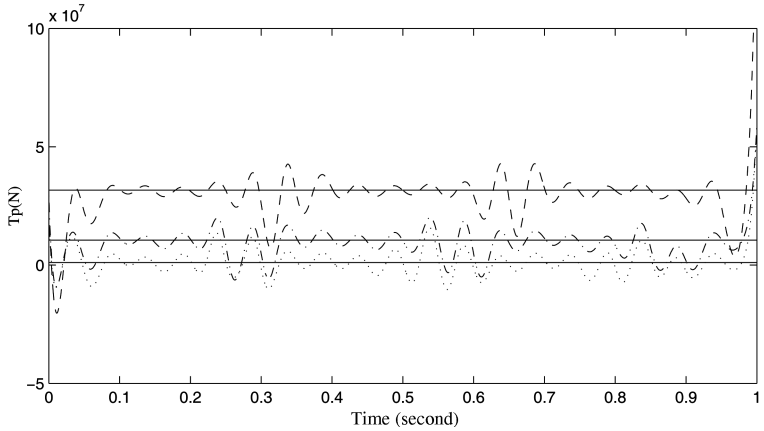


Fig. 3 Identification of different magnitude of prestress force (—— True, ----- $T_p = 0.3T_{cr}$, -·-·- $T_p = 0.1T_{cr}$, ····· $T_p = 0.01T_{cr}$)

### 4.4 Identification using impulsive excitation

An impulsive force is also used to identify the prestess force. It acts on the beam between $t$ = 0.05s to 0.15s. The magnitude of the prestress force is $0.1T_{cr}$ = 1.056 × $10^7$ N. The magnitude of the force is assumed to be 9500 N and it is applied at 7 m from the left support, which can be expressed as

$$f(t) = \begin{cases} 190000(t-0.05)N & (0.05 \le t \le 0.01) \\ 190000(0.15-t)N & (0.1 \le t \le 0.15) \end{cases}$$

The sampling frequency is 1000 Hz, and the first three modes and three displacement measurements evenly distributed along the beam are used in the identification. 10% noise is included in the identification. Fig. 4 shows that the identified prestress force is very close to the true one for most of the time history.

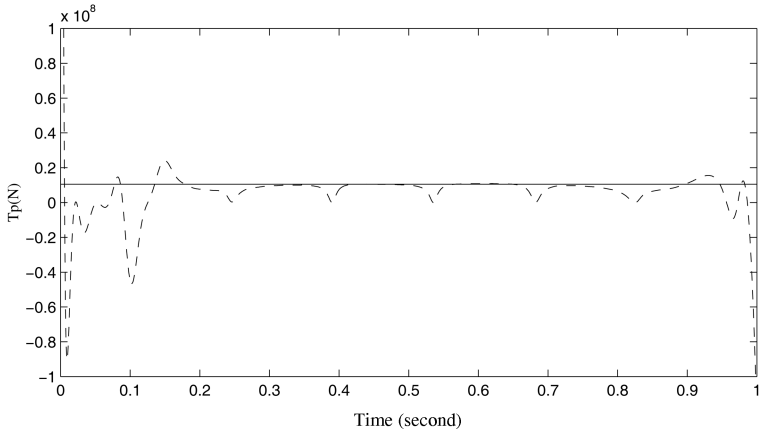


Fig. 4 Prestress force identified from impulsive force ( —— True, ----- Identified)

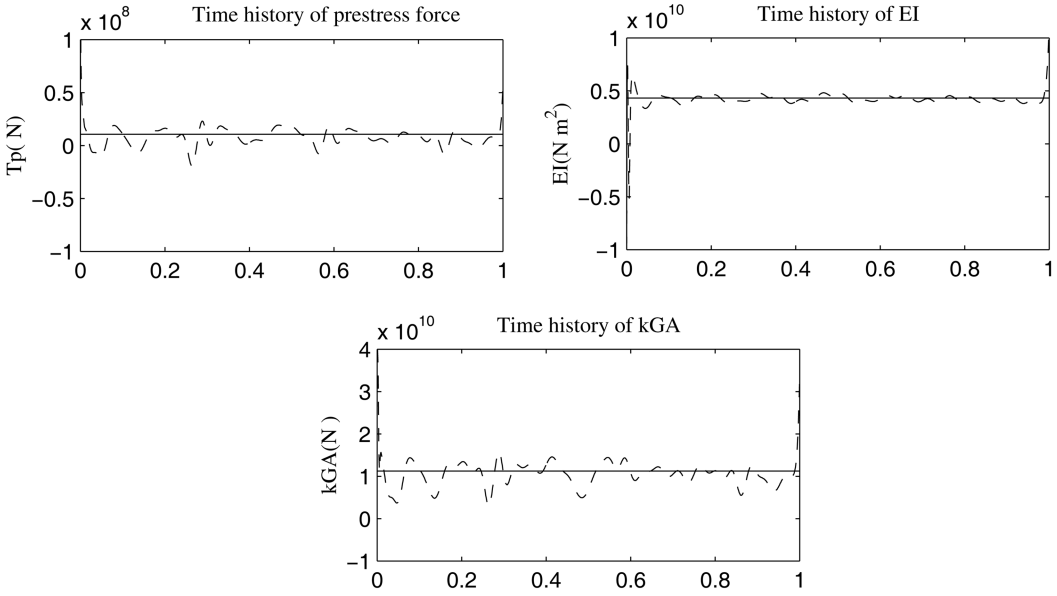


Fig. 5 Identification of $T_p$, $EI$ and $kGA$ ( —— True, ----- Identified)

### *4.5 Identification of the prestress force, the flexural rigidity and shearing rigidity of the beam*

The same system as for the last study is used here with a prestress force of $0.1T_{cr}$, and the flexural rigidity $EI$ and the shearing rigidity $kGA$ of the beam are $4.32 \times 10^9$ Nm$^2$ and $1.125 \times 10^{10}$ N, respectively. The sampling frequency is 1000 Hz, and the first three modes and three evenly distributed displacement measurements are used in the identification. 10% noise is also included in the identification.

Fig. 5 shows that the identified prestress force, flexural rigidity and shearing rigidity are fluctuating around the true values, which further verify the effectiveness of the proposed method with multiple parameters identification.

### *4.6 Comparison with the Euler-Bernoulli beam model*

Both Timoshenko beam model and Euler-Bernoulli beam model are used in the simulation study for a comparison purpose. The same prestressed beam is studied. The external exciting force is

$$f(t) = 8000[1 + 0.1\sin(10\pi t) + 0.05\sin(40\pi t)]N$$

and it is applied at 7 m from the left support to excite the lower few modes. White noise is added to the calculated displacements and strains to simulate the polluted measurements. 5% and 10% noise levels are considered. The first three modes are used in the calculation. Measured displacements at 1/4L, 1/2L and 3/4L are used in the identification. The sampling frequency is 1000 Hz. Table 2 shows the identified results from Timoshenko beam model and Euler beam model. It can be seen that the prestress force identified by Timoshenko beam model are more satisfactory than that identified by Euler-Bernoulli beam model.

Table 2 Error percentage in the identified force

| Prestress force | | 1% noise | 5% noise | 10% noise |
|---|---|---|---|---|
| 0.01Tcr | T | 172.6/(8.12 × $10^7$) | 184.0/(9.36 × $10^7$) | 190.7/(1.03 × $10^8$) |
| | E | 173/(7.77 × $10^7$) | 218.3/(1.1 × $10^8$) | 237.88/(1.37 × $10^8$ |
| 0.05Tcr | T | 77.87/(1.77 × $10^8$) | 78.8/(2.23 × $10^8$) | 83.89/(2.64 × $10^8$) |
| | E | 75.53/(1.79 × $10^8$) | 81.46/(2.16 × $10^8$) | 86.46((2.53 × $10^8$) |
| 0.1Tcr | T | 43.2/(2.06 × $10^8$) | 43.89/(2.14 × $10^8$) | 46.32/(2.47 × $10^8$) |
| | E | 46.37/(2.06 × $10^8$) | 48.33/(2.48 × $10^8$) | 50.29/(2.8 × $10^8$) |
| 0.2Tcr | T | 25.76/(2.57 × $10^8$) | 28.13/(3.09 × $10^8$) | 29.24/(3.59 × $10^8$) |
| | E | 31.02(3.03 × $10^8$) | 31.86(3.30 × $10^8$) | 32.8(3.66 × $10^8$) |
| 0.3Tcr | T | 17.05/(2.54 × $10^8$) | 17.3/(3.21 × $10^8$) | 19.16/(4.06 × $10^8$) |
| | E | 21.6/(3.43 × $10^8$) | 21.62/(3.48 × $10^8$) | 22.91/(3.56 × $10^8$) |

Note: (•) denotes the sum of squares error, *T* denotes the Timoshenko beam, *E* denotes the Euler-Bernoulli beam

## 5. Experimental verification

The proposed method is further verified with a simply supported prestress concrete beam in the laboratory. The experimental setup is shown diagrammatically in Fig. 6. It is 4.0 meters long with a 150 mm × 300 mm uniform cross-section and a clear span of 3.8 meters. A seven-wire straight strand was placed in a 57 mm diameter duct located at the centre of gravity of the beam cross-section throughout the length of the beam. The duct remains ungrouted such that the prestress force

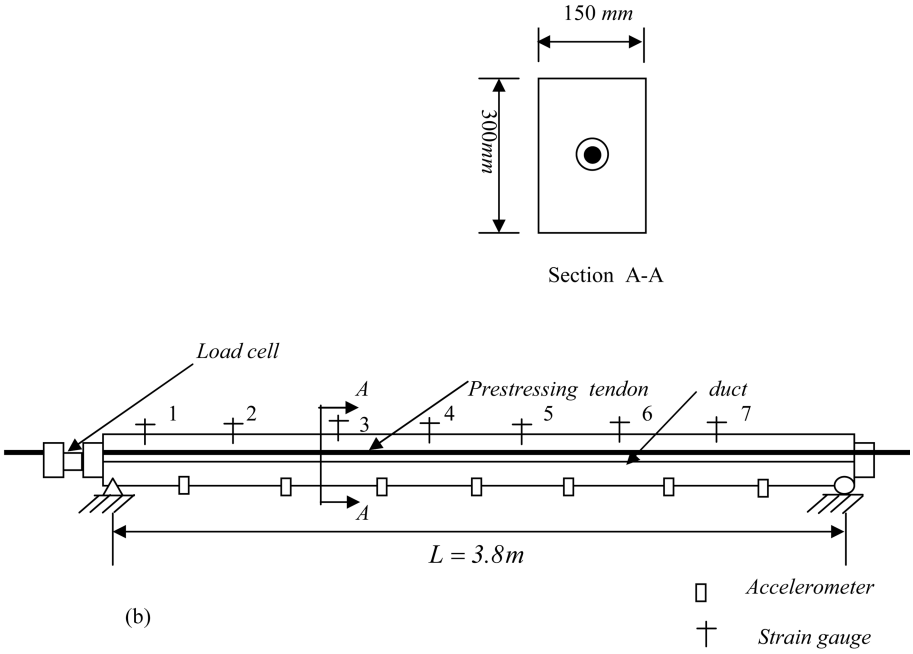


Fig. 6 Test setup for the prestressed concrete beam

can be monitored as a reference. The elastic modulus of concrete and the steel strand are respectively $31.5 \times 10^9$ N/m$^2$ and $194 \times 10^9$ N/m$^2$ and the mass density of concrete is $2.398 \times 10^3$ kg/m$^3$. The yield strength of the strand is 192 *kN*. The beam is instrumented with seven equally spaced strains to measure the dynamic strain responses of the beam.

### 5.1 Modal tests

Dynamic modal test is conducted on the concrete beam without prestress force first. The beam is excited with impacts from a Dytran Instruments 12 *lb* instrumented impulse hammer, model 5803A in the vertical direction at a fixed point 3L/8 from the left support. Seven accelerations located at 1L/8, 2L/8, 3L/8, 4L/8, 5L/8, 6L/8, 7L/8 are used for the modal test. A commercial data logging system INV303E and the associated signal analysis package DASP2003 are used in the data acquisition. One load cell is located at one end of the strand to measure the magnitude of prestress force applied on the concrete beam. After 180 *kN* prestress force is applied to the prestressing strand, another modal test is conducted on the prestressed beam. The first three natural frequencies of the intact beam and the prestressed beam are shown in Table 3. The experimental natural frequencies match the analytical natural frequencies well except the last one.

### 5.2 Identification of prestress force

The strain measurements from the forced vibration test are used for prestressed force identification. An impulsive force is applied with the impact hammer at 3L/8 from the left support of the beam. The sampling rate is 2000 Hz. Time histories of both the excitation force and the strains are recorded, and data obtained from the third and fourth strain gauges are used in the prestress force identification.

The flexural rigidity of the beam before prestressing is calculated as $1.0599 \times 10^7$ N-m$^2$. The beam is assumed to be simply supported. Rayleigh damping model is adopted in calculating the structural response, and the measured modal damping ratios for the first three modes are respectively 0.03, 0.14 and 0.12. The analytical modal frequencies are shown in Table 3.

After the beam is prestressed, the flexural rigidity of the beam section is calculated to be $1.060 \times 10^7$ N-m$^2$. The prestress force is identified using data from 0 second to 1.0 second after the hammer impact. Measured strains from the 3$^{rd}$ and the 4$^{th}$ strain gauges were used for prestress force identification. Fig. 7 shows the measured time history from the two strain gauges. The orthogonal polynomial function is used to remove the measurement noise. The measured modal

Table 3 Analytical and experimental natural frequencies (Hz)

| Mode No. | Analytical | | Experimental | |
|---|---|---|---|---|
| | Without prestress | With prestress | Without prestress | With prestress |
| 1 | 34.78 | 34.38 | 35.53 | 34.68 |
| 2 | 135.11 | 133.56 | 134.42 | 133.16 |
| 3 | 290.60 | 287.28 | 293.43 | 289.76 |
| 4 | 488.02 | 482.44 | 490.21 | 485.64 |
| 5 | 714.67 | 706.49 | 718.86 | 712.54 |

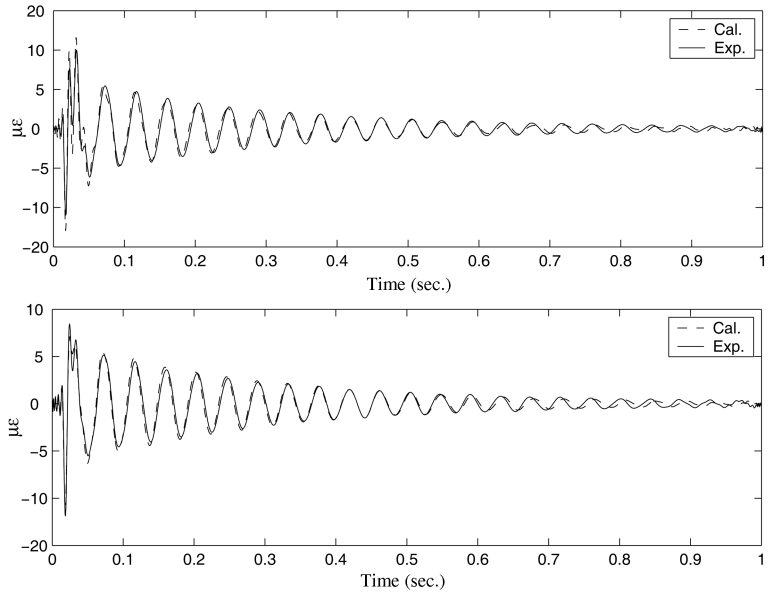


Fig. 7 Comparison on the calculated and experimental strain time hisories

damping ratios for the first three modes are 0.029, 0.14 and 0.11 respectively. The load cell at the end of the strand shows that the prestress force is 162.7 KN. The identified magnitude of the prestress force is 148.3 KN, the relative error is 8.9%. This shows the proposed method has the potential for practical prestress force identification.

## 6. Conclusions

A method is proposed to identify the prestress force in a Timoshenko beam with or without including the flexural rigidity and shearing rigidity of the beam. The noise effect on the measurements is improved using the orthogonal polynomial function. Both the sinusoidal and impulsive excitation could give very good results with the lower three measured modes and data obtained from three measuring points. It is shown that the proposed method is insensitive to the magnitude of force to be identified. Both numerical simulation and experimental work in this paper indicate that indirect measurement of the prestress force in the Timoshenko beam is feasible even under noisy environment.

## Acknowledgements

This work is supported in part by the NSFC (10772202), GDSF (07003680), Guangdong Province Science and Technology Program (2007B030402002) and the Start-up Fund for Fresh Teachers from Sun Yat-sen University (2006-39000-1131061).

## References

Abraham, M.A., Park, S.Y. and Stubbs, N. (1995), "Loss of prestress prediction on nondestructive damage location algorithms", *SPIE, Smart Struct. Mater.*, **244**, 60-67.

Abramovich, H. (1991), "Natural frequencies of Timoshenko beams under compressive axial loads", *J. Sound Vib.*, **15**7(1), 183-189.

Kim, J.T., Yun, C.B., Ryu, Y.S. and Cho, H.M. (2004), "Identification of prestress-loss in PSC beams using modal information", *Struct. Engi. Mech.*, **17**(3-4), 467-482.

Law, S.S. and Lu, Z.R. (2005), "Time domain responses of a prestressed beam and prestress force identification", *J. Sound Vib.*, **288**, 1011-1025.

Law, S.S. and Zhu, X.Q. (2000), "Study on different beam models in moving force identification", *J. Sound Vib.*, **234**, 661-679.

Miyamoto, A., Tei, K., Nakamura, H. and Bull, J.W. (2000), "Behavior of prestressed beam strengthened with external tendons", *J. Struct. Eng.*, ASCE, **126**(9), 1033-1044.

Newmark, N.W. (1959), "A method of computation for structural dynamics", *J. Eng. Mech. Div.*, ASCE, **85**(3), 67-94.

Saiidi, N., Douglas, B. and Feng, S. (1994), "Prestress force effect on vibration frequency of concrete bridges", *J. Struct. Eng.*, ASCE, **120**(7), 2233-2241.

## Appendix: Notation

The following symbols are used in this paper.

$\rho$ : mass density of the beam material
$A$ : cross-sectional area
$h_0$ : the height of the beam
$b$ : the width of the beam
$c$ : the viscous damping of the beam
$P(t)$ : the external exciting force
$E$ : Young's modulus
$G$ : shear modulus
$I$ : the second moment of inertia of the beam cross-section
$T_p$ : prestress force
$y(x, t)$ : transverse displacement of the beam
$\psi(x, t)$ : angle of rotation of cross-section
$Y_i(x)$, $\phi_i(x)$ : the assumed $i$th mode shape of the beam
$k$ : shear coefficient
$q_i(t)$ : modal co-ordinate
$[M]$ : modal mass matrix
$[C]$ : modal damping matrix
$[K]$ : modal stiffness matrix
$[K']$ : modal stiffness reduction due to the prestress force
$N$ : number of modes used
$N_f$ : number of the polynomial terms used
$\lambda$ : regularization parameter